PORTLAND CEMENT ASSOCIATION
RESEARCH AND DEVELOPMENT LABORATORIES

Development Department • Bulletin D106

HIGH STRENGTH BARS AS CONCRETE REINFORCEMENT, PART 8. SIMILITUDE IN FLEXURAL CRACKING OF T-BEAM FLANGES

By Paul H. Kaar

Reprinted from the Journal of the PCA
Research and Development Laboratories
Vol. 8, No. 2, 2-12 (May 1966)

HIGH STRENGTH BARS AS CONCRETE REINFORCEMENT, PART 8. SIMILITUDE IN FLEXURAL CRACKING OF T-BEAM FLANGES

By Paul H. Kaar

PORTLAND CEMENT ASSOCIATION
RESEARCH AND DEVELOPMENT LABORATORIES
5420 Old Orchard Road
Skokie, Illinois 60076

High Strength Bars as Concrete Reinforcement

Part 8. Similitude in Flexural Cracking Of T-Beam Flanges

By
Paul H. Kaar, Senior Development Engineer
Structural Development Section
Research and Development Laboratories
Portland Cement Association

SYNOPSIS

Control of flexural cracking in design is being studied as part of an experimental investigation of high strength reinforcing steel. *This Part 8 in a series of reports* concerns cracking on the top surface of T-beams subjected to negative bending moments. Using ¼, ½, and full-scale specimens, similitude of cracking is evaluated and the reliability of expressions for computation of crack width is discussed.

CONTROL OF FLEXURAL CRACKING

An experimental program at the PCA Laboratories, "High Strength Bars as Concrete Reinforcement," is being reported in a series of papers.(1-7)* Control of flexural cracking has so far been discussed in four of these reports, as follows:

Part 2, "Control of Flexural Cracking,"(2) evaluates flexural cracking in beams reinforced with American deformed bars in terms of design criteria developed by the European Concrete Committee (CEB).

Part 3, "Tests of Full-Scale Roof Girder,"(3) discusses the performance of a 60-ft precast roof girder.

Part 4, "Control of Cracking,"(4) reports flexural and shear cracking for both statically and dynamically loaded highway bridge beams. The CEB expression for flexural crack width was again studied, and new criteria were proposed for flexural crack control, recognizing that flexural crack width depends mainly on the reinforcing steel stress and the area of concrete surrounding each bar.

Part 7, "Control of Cracking in T-beam Flanges,"(7) contains a modification of the expression developed in Part 4 for crack width at the centroid level of the steel. The new expression is applicable to the tension face of a T-beam bridge in regions of negative moments, namely the roadway surface.

*Numbers in parentheses refer to references at end of paper.

Scope

The present paper completes the investigation of flexural crack control initiated in Part 7 for the slab flanges of T-beams. Such crack control is particularly important in detailing high strength reinforcement for continuous T-beam and box-girder bridges.

Tests of four T-beams subjected to negative bending moment are reported. Two full-scale specimens had proportions commonly used in grade separation bridges, and another two specimens were models of one of these built to ½ and ¼ scale.

Background

Since excellent summaries of previous investigations were published in 1965,(8-10) no further detailed review is needed here.

However, most previous tests were performed on relatively small specimens, ranging approximately from 1/4 to 1/2 scale of the members commonly used in North American bridge construction. It is the principal purpose of the investigation reported herein to evaluate application to full-scale members of design criteria previously derived from such small-scale tests. Possible effects of specimen size are therefore relevant.

In previous tests at the PCA Laboratories of a full-scale 60-ft roof girder[3] and a corresponding 1/2.6-scale model,[11] a significant difference in crack pattern was noted. At a steel stress of 30,000 psi, over 150 cracks intersected the main tension steel in the full-scale girder while the model had about 40 cracks. Still smaller test specimens, down to 1- by 2-in. reinforced mortar beams, frequently have only 5 to 10 cracks. This observed lack of similitude is contrary to findings of Borges and Lima[12] who concluded that "the similitude of the over-all view of the cracks is conspicuous . . . .". This question of similitude has two major implications:

(1) It has been noted in previous investigations[2] that crack width is inherently subject to a wide experimental scatter. If the total number of cracks increases with the scale used, the total range of observed crack widths for a beam normally increases, so that the presence of a few exceptionally wide cracks becomes more probable. On the other hand, for the same envelope of steel stress, a larger number of cracks should lead to narrower individual cracks. Which influence will govern crack width of full-scale members?

(2) Most available expressions for crack width are of such nature that computed width at a given steel stress is directly proportional to the scale of specimen considered. For example, in the expression originally developed by the European Concrete Committee,* crack width is proportional to the reinforcing bar diameter. However, in the formulas previously developed at the PCA Laboratories,[4,7] crack width is proportional to $\sqrt[4]{A}$, in which A is the average area of concrete surrounding each reinforcing bar, so the computed width is proportional to the square root of the scale.

*Eq. (7) in Ref. 2.

Crack Width Computation

Crack width at the tension face of a beam subjected to negative moment, that is, on the roadway surface of a T-beam, was previously[7] expressed as:

$$w_{t\,max} = 0.115\, R \sqrt[4]{A}\, f_s \times 10^{-6} \quad \ldots\ldots (1)$$

and

$$w_{t\,avg} = 0.077\, R \sqrt[4]{A}\, f_s \times 10^{-6} \quad \ldots\ldots (2)$$

in which

$w_{t\,max}$ and $w_{t\,avg}$ = maximum and average crack width, respectively, at the tension face, inches.

R = ratio of distances from the neutral axis to the tension face and to the centroid of the reinforcement.

A = average area of concrete surrounding each reinforcing bar; that is, area of concrete surrounding all tension reinforcing bars and having the same centroid as that of the total main reinforcement, divided by the number of bars, sq in.

f_s = service load steel stress, psi.

To be more explicit, the area of concrete surrounding each reinforcing bar is computed as twice the distance from the tension face to the centroid of the total reinforcement, multiplied by the width of the tension zone, and divided by the number of bars. When the reinforcement is well distributed in the flange, this computation also applies to T-beams under negative bending moments, the width of the tension zone being taken as the total width of the flange. When the tension steel centroid is located at middepth of the flange or below, A is taken as the product of flange thickness and width divided by the number of bars.

LABORATORY WORK

Test Specimens

The two full-scale T-beams are shown in Fig. 1. The transverse reinforcement in the roadway slab was No. 4 bars at 7 in. top and bottom. Beam No. 1 was also made in 1/2 and 1/4 scale. In all specimens the main reinforcing was of deformed bars.

The concrete used in the fabrication of the girders contained Type I portland cement and four to five percent entrained air. To avoid a variable tensile strength of the concrete dependent on maximum aggregate size, all concrete was made with the 3/8-in. maximum size aggregate necessary

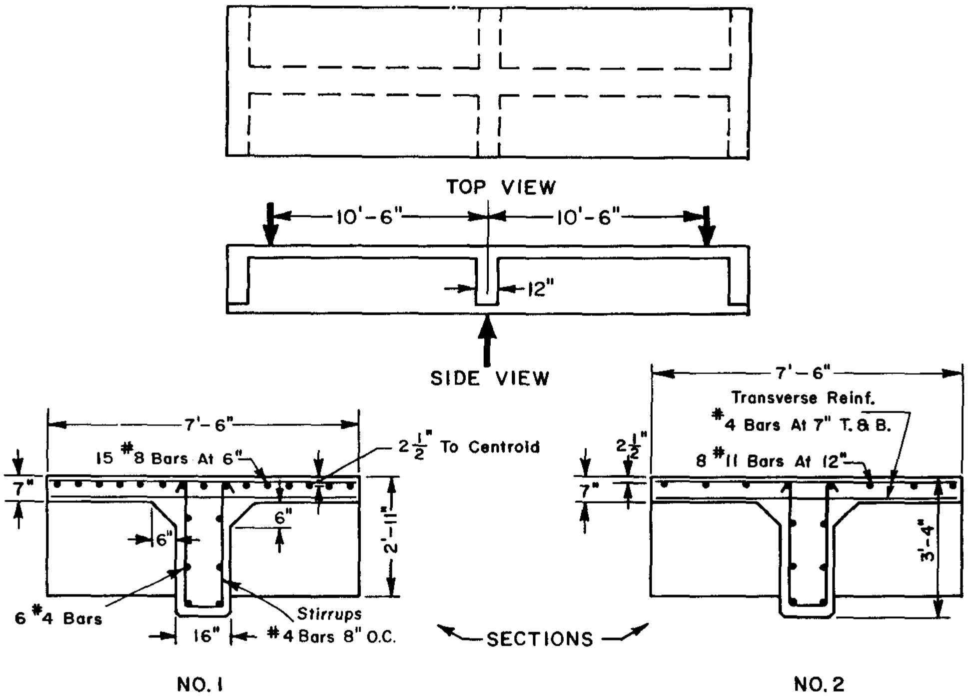

Fig. 1 — Full-Scale Specimens.

for the ¼-scale specimen. The ready-mixed concrete was delivered in four batches. The first batch was placed in the stems of the three scaled girders. After allowing the stems to set for two hours for initial settlement, the second batch was used in casting the decks. The second full-scale specimen (No. 2) was cast separately using two batches. Moist curing under a plastic sheet took place at 70 F for the first three days after casting. The specimens were tested 34 to 38 days after casting.

Concrete test specimens were taken at intervals during the casting of the girders. Compression and tension test results, which are the averages for two to seven specimens, are shown in Table 1. Properties and strength data for the T-beams are given in Table 2.

Test Method

The T-beam specimens were loaded by hydraulic rams under the center diaphragm and were restrained by tie rods near their ends. Figs. 2 to 4 show the loading arrangements in which a negative moment service condition is simulated. At intervals during loading, the width of each flexural crack was measured at the flange edges, above each reinforcing bar, and between adjacent bars by a graduated 40-power microscope. Hence, for the ¼-, ½-, and ¼-scale specimens with 15 longitudinal reinforcing bars, 31 measurements were made of each crack traversing the full flange width. The number of readings per crack taken in the same manner for specimen No. 2, with 8 deck reinforcing bars, was 17.

Steel Stress

The loading system causes a variable steel stress throughout the member. Eqs. (1) and (2) give crack width as proportional to the reinforcing bar stress. The steel stress at a cracked section varies almost linearly with the applied load, since during loading of the specimens the internal lever arm changes only slightly between service load and ultimate strength. The steel stress at any stage before yield may thus be approximated by

TABLE 1—CONCRETE STRENGTHS

Strength	Full- and Reduced-Scale Specimens, No. 1		Full-Scale Specimen, No. 2	
	Girder	Deck	Girder	Deck
Compression, psi	5520	5030	4580	5160
Tension, psi:				
Modulus of Rupture Test	620	570	520	570
Direct Tension Test	430	440	—	430
Split Cylinder Test	500	480	500	560

TABLE 2—PROPERTIES AND STRENGTH OF T-BEAMS

Item	Full-Scale No. 1	½-Scale No. 1	¼-Scale No. 1	Full-Scale No. 2
Number and size of bar	15 No. 8	15 No. 4	15 No. 2	8 No. 11
Concrete strength, psi	5520	5520	5520	4580
Tension steel area, sq in.	11.85	3.00	0.75	12.48
Concrete area surrounding each bar, sq in.	30.0	7.5	1.875	60.0
Net reinforcement ratio (p-p'), %	1.91	1.93	1.93	2.01
Net reinforcement index (q-q')	0.27	0.23	0.22	0.25
Ratio R	1.11	1.11	1.11	1.12
Reinforcement yield, ksi	79.1	66.2	64.0	57.7
Ultimate moment M_{test}, in. kips	24,430	3,540	420	23,960
M_{test}/M_{calc}	0.83*	1.10	1.07	1.04
Maximum measured concrete compressive strain	0.0028*	0.0042	0.0047	0.0043

*This beam failed in shear, all others in flexure.

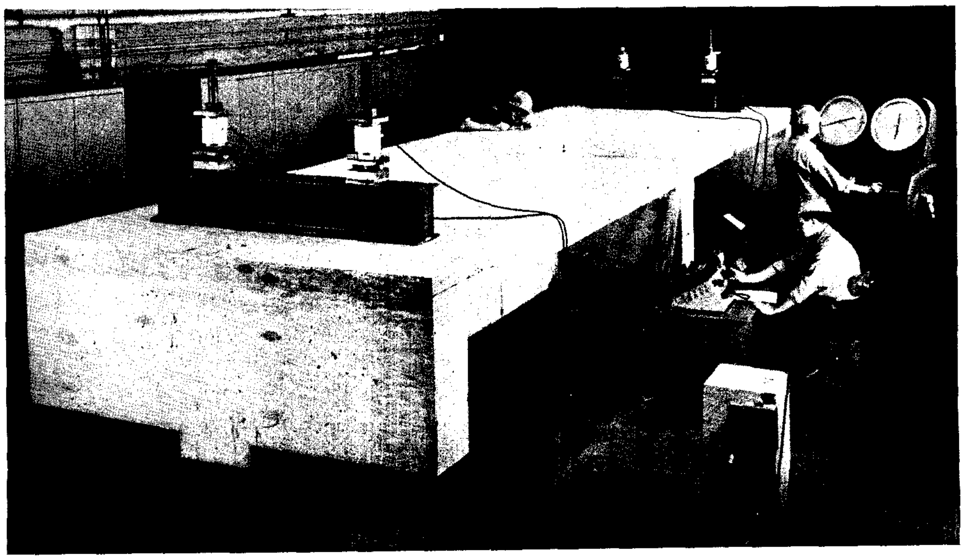

Fig. 2—Test of Full-Scale T-Beam.

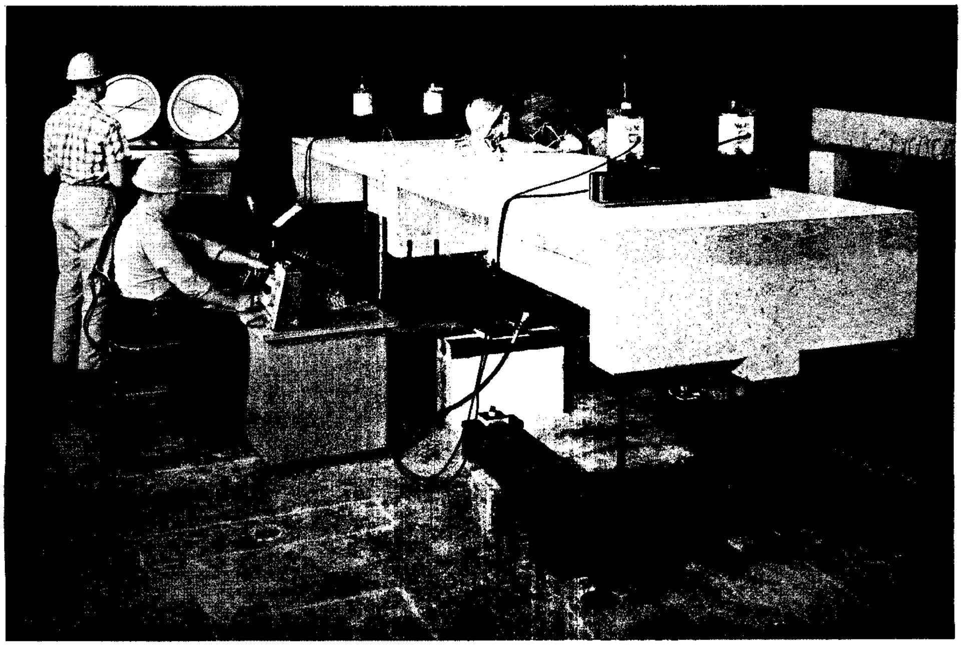

Fig. 3 — Test of ½-Scale T-Beam.

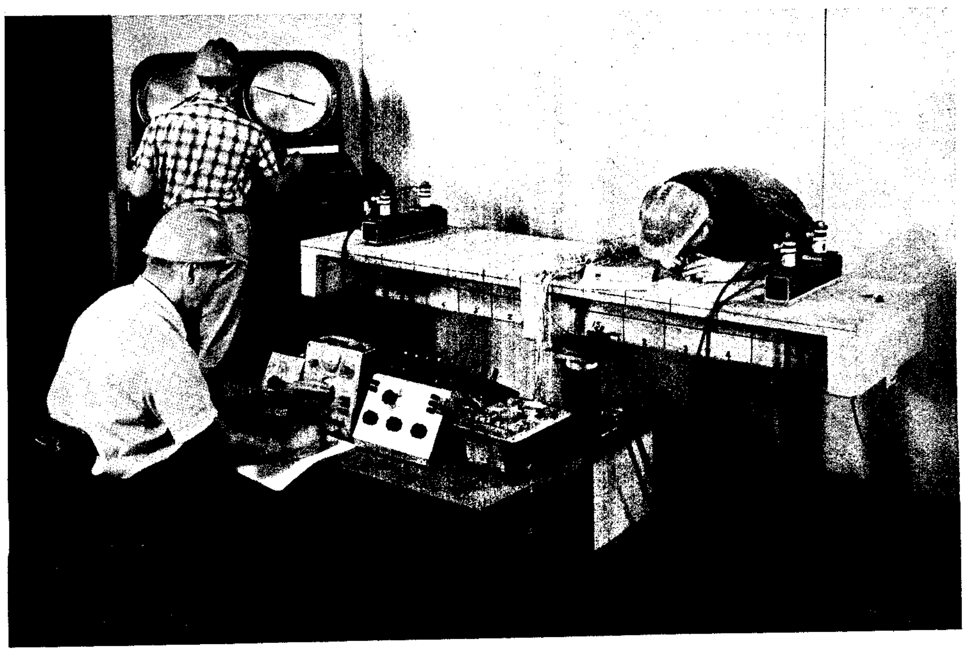

Fig. 4 — Test of ¼-Scale T-Beam.

$$f_s = f_y M_s/M_u \ldots\ldots\ldots\ldots (3)$$

in which

M_s = moment at loading in question

M_u = ultimate moment computed on the basis of the steel yield strength by applicable procedures of the 1963 ACI Building Code.

The reinforcing steel stress at each crack location and at each load level was computed by Eq. (3). In computing the moment acting at each crack, it was assumed that the reaction load was dispersed at 45 degrees from the edge of the support bearing plate upward to the neutral axis, as shown in Fig. 5. Test data of steel strains along the longitudinal main reinforcement for girders of similar proportions have shown a variation corresponding reasonably well with the variation of moment described.

Strain gages were attached to each reinforcing bar directly above one face of the center diaphragm. To insure a flexural crack traversing the strain gages, an internal strip of sheet metal was embedded in each deck in line with the strain gages. Average reinforcing bar stresses derived from these gages are compared in Table 3 with the bar stress computed by Eq. (3). Agreement of results is quite good.

TEST RESULTS

Data related to the ultimate strength of the test beams are given in Table 2. As is usual in tests of this nature, the observed ultimate moments exceeded computed values somewhat. Both full and small-scale specimens produced reliable data on ultimate strength. The main reinforcement for full-scale beam No. 1 had a higher yield point than expected (as shown in Table 2), and its strength was therefore governed by shear.

Load-deflection diagrams for full-scale beam No. 1 and its two models were practically identical when deflection divided by scale was plotted versus concentrated load divided by the square of the scale.

Crack Patterns

The crack patterns for beam No. 1 and its two models are shown in Fig. 6 for a loading producing a steel stress of 30,000 psi at the center diaphragm. It is seen that the nature of the crack patterns is the same regardless of scale, but the total number of

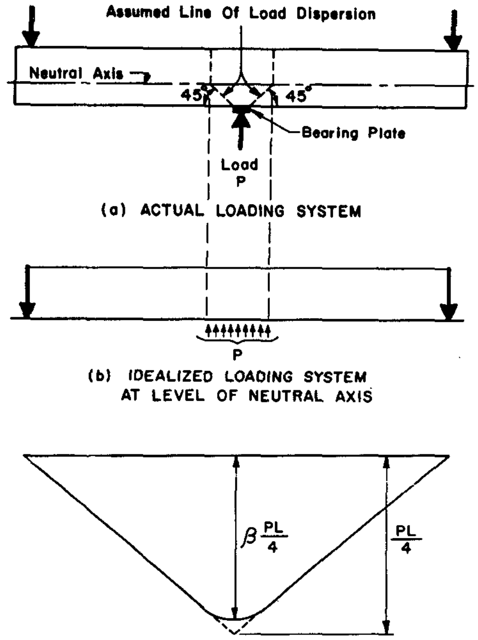

Fig. 5 — Bending Moment in Beams.

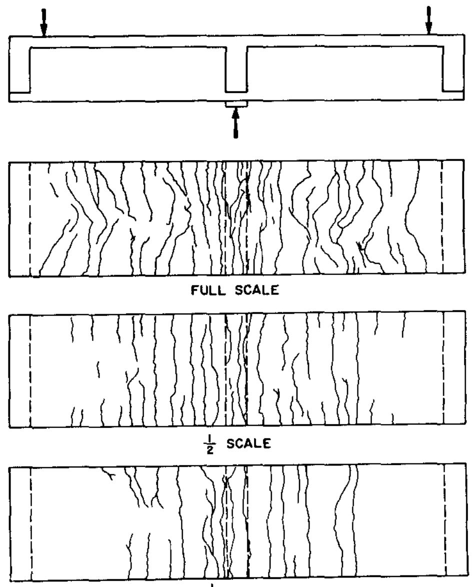

Fig. 6 — Crack Patterns on Roadway Surface, No. 1 Design, Steel Stress 30 KSI at Diaphragm.

cracks is greater for the full-scale than for the 1/4-scale member. This confirms previous findings at the PCA Laboratories indicating that similitude with respect to crack formation does not hold true between large specimens and reduced scale models. No relation was apparent between transverse bar and flexural crack spacing.

Crack Width Across Deck

Distribution of stress in the main reinforcement of full-scale beam No. 2 at the center diaphragm is plotted in Fig. 7. It is seen that, for the uniform bar spacing used, there is a concentration of steel stress over the girder web. This indication of shear lag, common in T-beams, was observed for all four specimens of this study and also in previous tests of a two-span T-beam bridge.[13] Though this behavior indicates that plane sections perpendicular to the axis of the test beams do not remain plane after bending, little influence of this could be detected in terms of crack width variation across the width of the T-flange.

TABLE 3—STRESS IN DECK REINFORCEMENT

T-Beam Specimen	Load Stage	Reinforcing Bar Stress, ksi	
		Eq. (3)	Strain Gages
Full Scale No. 1	1	11.6	6.3
	2	15.6	14.1
	3	22.2	21.1
	4	29.0	27.9
	5	37.8	40.1
	6	47.3	48.3
	7	55.0	56.9
1/2 Scale No. 1	1	12.8	10.7
	2	19.1	19.4
	3	26.0	27.6
	4	34.4	36.6
	5	42.6	45.4
	6	50.0	53.0
1/4 Scale No. 1	1	17.1	17.0
	2	21.2	20.8
	3	25.0	25.6
	4	28.8	31.2
	5	34.4	34.9
	6	40.2	43.7
	7	47.6	52.1
Full Scale No. 2	1	4.0	1.9
	2	6.8	5.7
	3	10.2	13.4
	4	17.7	20.0
	5	24.3	26.4
	6	33.0	34.8
	7	40.8	41.4
	8	46.9	47.6
	9	49.5	49.4
	10	52.6	51.7
	11	55.8	55.8

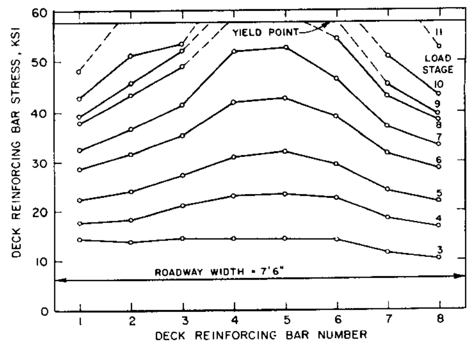

Fig. 7 — Variation of Steel Stress Across Roadway, Full-Scale Beam No. 2.

Crack Width Along Beam Length

Crack widths along the length of the four T-beam specimens are plotted in Fig. 8 for load stages giving a maximum steel stress over the center diaphragm somewhat below 30,000 psi. Only crack widths measured directly over each longitudinal reinforcing bar are considered. The maximum width is indicated for each crack, and a horizontal mark on the bars of the graph represents a crack width exceeded in only 15 percent of the measurements made. Absence of a horizontal mark indicates uniform width.

Plots of the maximum crack widths predicted by Eq. (1) are added to Fig. 8. For the loading arrangement used, the reinforcing steel stress and consequently the predicted crack width varies from zero at the beam ends to a maximum at the center.

Considering the ± 50 percent scatter usually associated with observed crack widths, the agreement between observed and computed crack width is satisfactory. The tendency is seen, however, for maximum crack width to be underestimated for large specimens and overestimated for small ones. It is believed that two scale effects combine to cause this. Since for a given envelope of steel stress the total number of cracks is less for the small specimens, the individual cracks should be wider. On the other hand, for the greater number of cracks in the large specimens the presence of a few exceptionally wide cracks becomes more probable. This latter effect seems to predominate.

Probability Distribution of Crack Widths

As mentioned earlier, each crack traversing the T-flange was measured at numerous locations. Futhermore, measurements were made at 6 to 11 load stages, so a computed steel stress at the location involved corresponds to each crack width measurement. Accordingly, crack widths corresponding to a given steel stress were first observed near the center diaphragm, but this same steel stress occurred later for higher load stages at other cracks located further toward the ends of the specimens. By considering all cracks and all load stages, crack width observations were sorted into corresponding steel stress ranges, such as from 27.5 to 32.5 ksi for an average stress level of 30 ksi. In this manner, 15 to 20 cracks and several hundred separate width measurements were considered for each average steel stress level. Such groups of crack widths were then sorted by electronic computation for preparation of probability distribution curves such as those shown in Figs. 9 and 10.

Fig. 9 concerns crack width at an average steel stress of 30 ksi. The probability distribution indicates, for example, that 85 percent of the crack widths measured between bars for full-scale beam No. 2 at a steel stress of 30 ksi were 0.014 in. or less. Widths observed directly above and midway between reinforcing bars are considered separately. The cracks were wider between bars, as expected, but this widening could be noticed only by examining groups of numerous individual measurements. Fig. 9 shows that the widening amounts to only about 0.0005 in. for the No. 1 full-scale and model specimens, while it was 0.001 to 0.002 in. for the No. 2 beam. This shows an advantage for closely spaced bars.

Fig. 10 illustrates the effect of steel stress on crack width for full-scale beam No. 1. As would be expected, crack width is approximately proportional to steel stress.

Figs. 9 and 10 both show that crack width at a given steel stress varies widely. For example, for full-scale beam No. 1 at a steel stress of 30 ksi, the crack width over bars varies from 0.001 to 0.015 in. It is seen that the range of crack width variation increases with size of specimen. The drawn

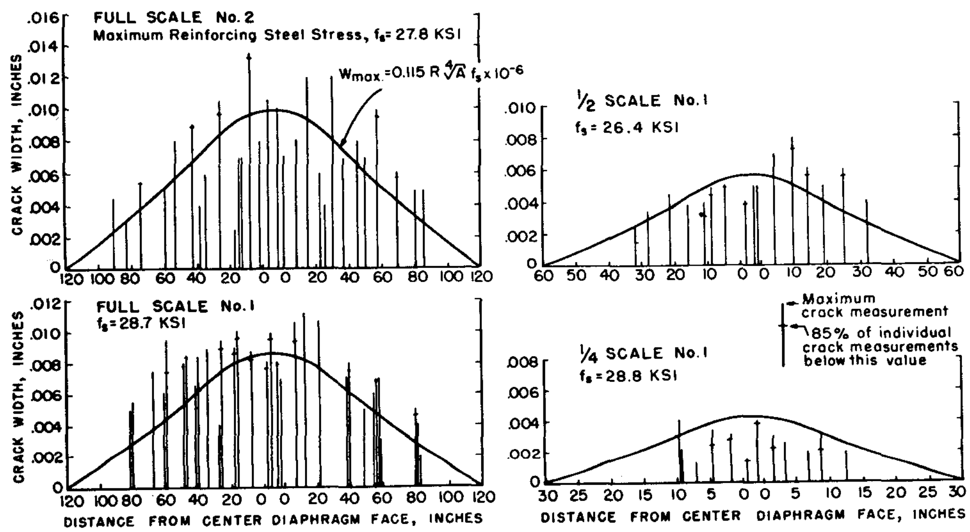

Fig. 8—Variation of Crack Width Along Beam Length.

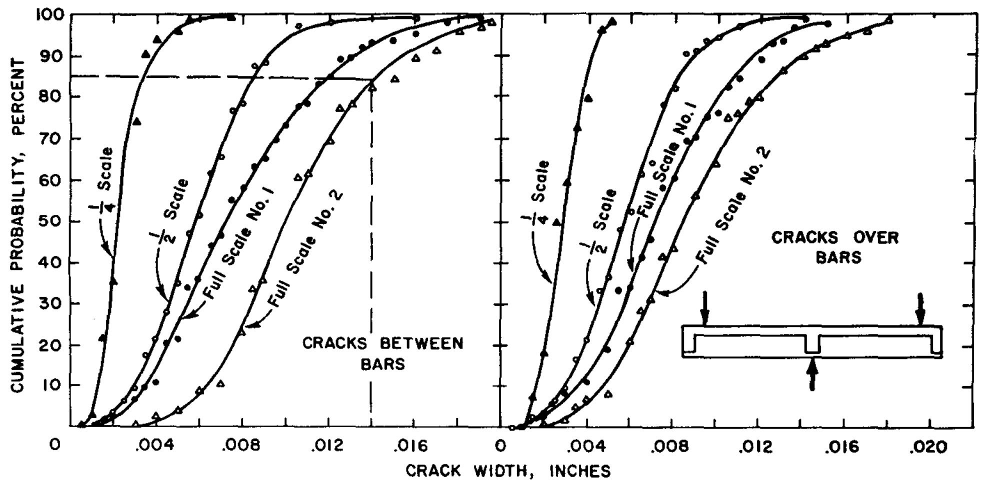

Fig. 9 — Probability Distribution of Crack Width, 30 KSI Average Steel Stress.

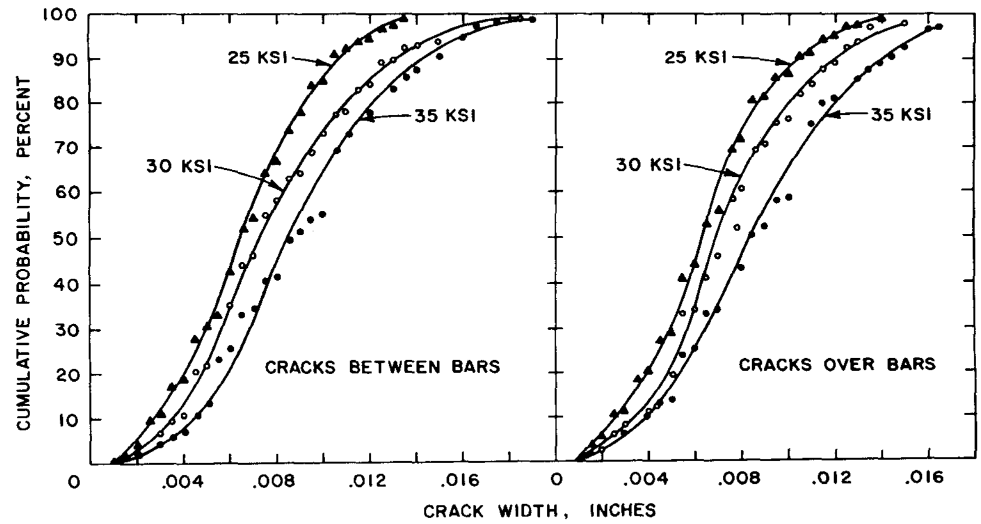

Fig. 10 — Probability Distributions, Full-Scale Beam No. 1.

out shapes of the "S" distribution curves near 100 percent probability represent measurements across exceptionally wide cracks. Fifteen measurements were made over the reinforcing bars for each crack crossing the entire width of the T-flange for the No. 1 beams. The exceptionally wide crack observations, therefore, stem from a "dual maximum", the widest point on the widest crack.

Some pertinent crack width data are summarized in Table 4. While average and median crack width agree reasonably well with values computed by Eq. (2), the absolute maxima of observed width considerably exceed those computed by Eq. (1) except for the ¼-scale specimen. The widths computed by Eq. (1) correspond more realistically to widths having a probability of 70 to 85 percent in Fig. 9.

Control of Cracking in Design

In practical design, computed maximum crack widths must not exceed limiting values for crack widths that can be tolerated without significant corrosion of the reinforcing steel. Selection of such limiting crack widths for various exposure conditions is generally made on the basis of exposure tests involving relatively small specimens.[14] Observed rusting of reinforcing bars is classified as none, slight, significant, and serious. The occurrence of such rusting in numerous observations is expressed as probability distribution functions with respect to crack width. Limiting crack widths are then usually chosen as those corresponding to a 10-percent probability of significant rust.

When such limiting crack widths are applied in design of large members, such as the full-scale beams involved in the present investigation, it seems unreasonable to consider the absolute maximum in computation of crack width, that is, 100-percent probability in Fig. 9. Design expressions should rather be based on observed widths having a 70- to 85-percent probability. Such widths are plotted in Fig. 11 as a function of the concrete area, A, for all four beams tested. Comparison is made with Eq. (1) and also with a modification of the CEB equation* involving the square root of the concrete area surrounding each bar.

Though Eq. (1) yields computed widths corresponding to the relatively low probability of 70 percent for observed width, the test data do indicate a trend following $\sqrt[4]{A}$ rather than $\sqrt{A}$. In other words, for the same specimen made to various scales, crack width is proportional to the fourth root of A, and hence to the square root of the scale. This confirms findings in Parts 4 and 7 of this series.

*Eq. (9) in Part 4 of this series.[4]

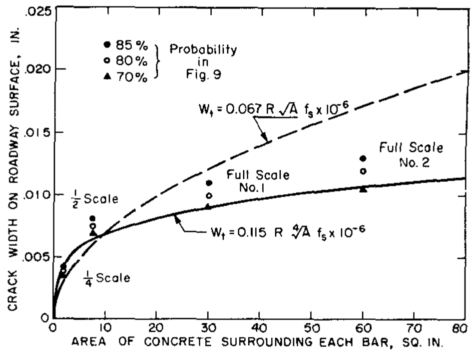

Fig. 11 — Crack Width over Bars, 30 KSI Average Steel Stress.

CONCLUSIONS

▮ T-beams made in various sizes from ¼ to full scale did not have identical crack patterns under negative moment loading to the same maximum steel stress. The crack patterns were of the same general nature, but the total number of cracks was greater for the larger members.

▮ Probability distribution curves for crack width indicate that the presence of a few exceptionally wide cracks is more likely for full-size bridge beams than for small-scale models.

▮ Though the absolute maximum values for observed crack width at isolated points considerably exceeded those computed by Eq. (1), this equation represents the effect of scale quite well, indicating that crack

TABLE 4—CRACK WIDTH MEASURED OVER BARS, 30-KSI AVERAGE STEEL STRESS

Specimen	Crack Width, thousandths of an inch						
	Maximum Width Observed	Width from Fig. 9		Maximum Computed by Eq. (1)	Average Width Observed	Median Width, Fig. 9	Average Computed by Eq. (2)
		85%	70%				
Full-Scale No. 1	15	11	9	9	7	7	6
½-Scale	14	8	7	6	6	5	4
¼-Scale	5	4	3	4	3	3	3
Full-Scale No. 2	18	13	10	11	9	8	7

width is proportional to square root of the scale factor. About 70 percent of the crack widths observed directly over longitudinal reinforcing bars were equal to or less than those computed by Eq. (1). The cracks were slightly wider between the bars.

The findings reported here confirm those given in Parts 4 and 7 of this series. To achieve crack control in T-beam flanges, the reinforcing steel should be well distributed throughout the flange. The smallest practical spacing should be used between individual reinforcing bars.

REFERENCES

1. Hognestad, Eivind, "High Strength Bars as Concrete Reinforcement, Part 1. Introduction to a Series of Experimental Reports," *Journal of the PCA Research and Development Laboratories,* **3,** No. 3, 23-29 (September 1961); *PCA Development Department Bulletin D52.*
2. Hognestad, Eivind, "High Strength Bars as Concrete Reinforcement, Part 2. Control of Flexural Cracking," *Journal of the PCA Research and Development Laboratories,* **4,** No. 1, 46-63 (January 1962); *PCA Development Department Bulletin D53.*
3. Gaston, J. R. and Hognestad, Eivind, "High Strength Bars as Concrete Reinforcement, Part 3. Tests of Full-Scale Roof Girder," *Journal of the PCA Research and Development Laboratories,* **4,** No. 2, 10-23 (May 1962); *PCA Development Department Bulletin D54.*
4. Kaar, P. H. and Mattock, A. H., "High Strength Bars as Concrete Reinforcement, Part 4. Control of Cracking," *Journal of the PCA Research and Development Laboratories,* **5,** No. 1, 15-38 (January 1963); *PCA Development Department Bulletin D59.*
5. Pfister, J. F. and Mattock, A. H., "High Strength Bars as Concrete Reinforcement, Part 5. Lapped Splices in Concentrically Loaded Columns," *Journal of the PCA Research and Development Laboratories,* **5,** No. 2, 27-40 (May 1963); *PCA Development Department Bulletin D63.*
6. Pfister, J. F. and Hognestad, Eivind, "High Strength Bars as Concrete Reinforcement, Part 6. Fatigue Tests," *Journal of the PCA Research and Development Laboratories,* **6,** No. 1, 65-84 (January 1964); *PCA Development Department Bulletin D74.*
7. Kaar, P. H. and Hognestad, Eivind, "High Strength Bars as Concrete Reinforcement, Part 7. Control of Cracking in T-Beam Flanges," *Journal of the PCA Research and Development Laboratories,* **7,** No. 1, 42-53 (January 1965); *PCA Development Department Bulletin D84.*
8. Lash, S. D., and Blackwell, W., "High Strength Reinforcement in Reinforced Concrete Beams, Part 1: A Selective Bibliography," *O.J.H.R.P. Report No. 37,* Department of Civil Engineering, Queen's University, Kingston, Ontario (February 1965), 21 pages.
9. Lash, S. D., MacLeod, N., and Blackwell, W., "High Strength Reinforcement in Reinforced Concrete Beams, Part 2: Crack Widths, Deflections, Fatigue Strength," *O.J.H.R.P. Report No. 38,* Department of Civil Engineering, Queen's University, Kingston, Ontario (June 1965), 86 pages.
10. Reis, Elmer E., Jr., Mozer, John D., Bianchini, Albert C., anl Kesler, Clyde E., "Causes and Control of Cracking in Concrete Reinforced with High Strength Steel Bars — A Review of Research," *Engineering Experiment Station Bulletin 479,* University of Illinois, Urbana (August 1965), 61 pages.
11. Gaston, J. R., and Hognestad, Eivind, "Precast Concrete Girders Reinforced with High Strength Deformed Bars," *Journal of the American Concrete Institute* (October 1958), *Proceedings,* **55,** 469-484 (1958-59); *PCA Development Department Bulletin D24.*
12. Borges, J. Ferry, and Lima, J. Arga E., "Crack and Deformation Similitude in Reinforced Concrete," *RILEM Bulletin,* No. 7, 79-90 (June 1960).
13. Mattock, A. H., and Kaar, P. H., "Precast-Prestressed Concrete Bridges, 6. Tests of Half-Scale Highway Bridge Continuous over Two Spans," *Journal of the PCA Research and Development Laboratories,* **3,** No. 3, 30-70 (September 1961); *PCA Development Department Bulletin D51.*
14. Rehm, G., and Moll, H. L., "Tests to Study the Effect of Crack Width on Corrosion of Reinforcement in Concrete Members," and Moll, H. L., "Corrosion of Steel in Concrete," *Deutscher Ausschuss für Stahlbeton, Heft 169,* Wilhelm Ernst und Sohn, Berlin (1964), 61 pages. In German with French and English summaries.

PCA.R&D.Ser.1219-2

Bulletins Published by the Development Department Research and Development Laboratories of the Portland Cement Association

D100—"Index of Development Department Bulletins D1-D99. Annotated List with Author and Subject Index."

Published by Portland Cement Association, Research and Development Laboratories, Skokie, Illinois (1966).

D101—"Rotational Capacity of Hinging Regions in Reinforced Concrete Beams," by ALAN H. MATTOCK.

Reprinted from FLEXURAL MECHANICS OF REINFORCED CONCRETE, *Proceedings of the International Symposium, Miami, Fla. (November 1964)* pages 143-181, joint sponsorship. Copyrighted 1965 by American Society of Civil Engineers.

D102—"Tests of Partially Prestressed Concrete Girders," by DONALD D. MAGURA and EIVIND HOGNESTAD.

Reprinted from the *Journal of the Structural Division, Proceedings of the American Society of Civil Engineers, Proc. Paper 4685,* **92,** ST 1, 327-350 (February 1966).

D103—"Influence of Size and Shape of Member on the Shrinkage and Creep of Concrete," by TORBEN C. HANSEN and ALAN H. MATTOCK.

Reprinted from *Journal of the American Concrete Institute* (February 1966); *Proceedings* **63,** 267-290 (1966).

D104—"Cast-in-Place Concrete Residences With Insulated Walls," by HARRY L. SCOGGIN.

Reprinted from *Journal of the PCA Research and Development Laboratories,* **8,** No. 2, 21-29 (May 1966).

D105—"Tensile Testing of Concrete Block and Wall Elements," by RICHARD O. HEDSTROM.

Reprinted from *Journal of the PCA Research and Development Laboratories,* **8,** No. 2, 42-52 (May 1966).

D106—"High Strength Bars as Concrete Reinforcement, Part 8. Similitude in Flexural Cracking of T-Beam Flanges," by PAUL H. KAAR.

Reprinted from *Journal of the PCA Research and Development Laboratories,* **8,** No. 2, 2-12 (May 1966).

Printed in U.S.A.